A SUBARRAY-BASED ANTENNA DESIGN FOR SATELLITE COMMUNICATIONS GROUND TERMINALS IN KA BAND

Federico Boulos, Stefano Caizzone, Andreas Winterstein
German Aerospace Center (DLR), Wessling, Germany
Federico.Boulos@dlr.de, Stefano.Caizzone@dlr.de, Andreas.Winterstein@dlr.de

Abstract

In recent years, non-terrestrial networks have experienced an exponential growth due to the launch of several new mega-constellations dedicated at communication services. Global connectivity, IoT and future integration with the terrestrial network appear as key technological trends that will shape the design of satellite systems in the next decade. With the new generation of HTS (high-throughput satellites), able to provide terabit of throughput for satellite, the ground side is becoming the bottleneck of the whole system. In particular, the ground terminal has to cope with strong and contrasting requirements: at high level, ground terminals will be required to communicate with satellites both in GEO and LEO orbit while on mobile platforms (*e.g.* train, aircraft, cars). This provokes the need for complex designs, capable of meeting the technical challenges associated with the high level requirements. However, the market penetration of such ground terminals, key to the overall success of these new communication systems, is strongly dependent on their SWAP-C (Size, Weight, Power and Cost): a strong push from the market is going into the direction of small and low-cost terminals, clearly contrasting with the complex design needed from a technical side. Among the several available antenna technologies, requirements such as multi-beam, wide scan-range, tracking accuracy and high-reconfigurability, make phased array antennas a promising solution from a technical point of view. In a phased array antenna multiple radiators are employed, each one supplied by a transmit/receive module (TRM) manipulating the amplitude and phase of the incoming/outcoming signal. High reconfigurability of the radiation pattern and the fitting of the user specifications, like directivity, sidelobe level (SLL) and half power beamwidth (HPBW), is then achieved by the proper selection of the amplitude/phase values provided to the different elements defining the antenna aperture. On the other hand, in contrast to the several benefits and features that phased array antennas can satisfy, the high number of elements required, the high cost and power consumption of this technology makes it not suitable yet for the consumer market (*i.e.* for a scenario where the final cost is an important key factor).
To overcome the main issues of phased array antennas, trade-off solutions have to be found, capable of combining the advantages of the phased array technology while minimizing their disadvantages. In this context, the subarray approach appears very promising: a TRM is shared among different elements bringing to simplification of the beamforming network (BFN), reduction of the power consumption and of the total number of RF chains. Each subarray is considered as an independent modular radiating element. Such element can be used as a tile in the overall antenna aperture and different sizes can be adopted to optimize the performance for a specific scenario.

The following paper presents the recent developments of a subarray-based antenna for SatCom applications conducted at the Institute of Communications and Navigation of the German Aerospace Center (DLR). The single antenna and subarray models, designed to work at f=19.95 [GHz] with an instantaneous bandwidth of 500 [MHz] and supporting simultaneous left-hand and right-hand circular polarization (LHCP, RHCP), are shown at first in simulation and then manufactured prototypes are presented. The developed technology is finally validated by measurements in DLR's compact test range anechoic chamber and results from the measurements are compared with simulated ones. Array antenna pattern is computed numerically with the subarray as element pattern and the results achieved are compared with the achievable results from a fully-populated reference solution.

1. Introduction

Phased arrays have found in the recent years a strong interest in many scenarios as communications, GNSS, automotive, military applications, remote sensing and in many other fields. Initially available for military radars, in the last years phased arrays found a big tentative of commercialization also for civil purposes. Indeed, with the exponential growth of space-based communications services, phased arrays became an attractive solution for consumer and enterprise market to address the strong requirements that a ground terminal in space communications has to deal as wide-angle continuous steering, high-reconfiguration, instantaneous tracking of multiple satellites (both in GEO and LEO orbit) and not least the fitting of the user specifications in terms of directivity, HPBW, SLL and mask-matching. In a phased array antenna, different elements are employed, usually arranged on a square-lattice grid but depending by the applications also hexagonal and triangular lattice grids can be adopted. Each antenna element is equipped with a transmit/receive module (TRM) controlling the amplitude and phase of the incoming/outcoming signal. However, for the high number of antennas that phased array requires, a very large aperture with high power consumption and manufacturing cost is required. The interest in commercialization of phased array for the consumer market has permitted to push the development of ASIC (*i.e.* application-specific integrated circuit) devices, addressing power consumption and manufacturing costs with clear benefits on miniaturization and simplification of antenna feeding architecture (*e.g.* antenna in package solutions). At the same time unconventional suboptimal approaches are being investigated trying to mitigate the SWAP-C factor. Solutions based on thinned/sparse array approach remove elements from the aperture reducing the number of RF chains: the mentioned solution has proven to be very effective also in the interference suppressions [1] [2] and adaptively thinned array are realized by connecting the antenna elements to RF switches. Several approaches were used for the synthesis of thinned array mainly based on stochastic natural-inspired algorithm as genetic algorithm (GA) [3] or particle swarm optimization [4] but other different techniques were employed as the iterative FFT techniques [5]. On the other hand, thanks to their modularity which simplifies the mass production, subarray approach results as a promising suboptimal solution based on reduction of RF chains by clustering physically contiguous antenna elements. In a subarray a TRM is shared among different antenna elements with a strong reduction in the power consumption, number of control points and antenna weights. Trade-off solutions which takes care of antenna design complexity and requirements satisfaction are designed accordingly to several synthesis methodologies to mitigate the undesired reduction in the quantization levels which as major effect causes grating lobes in the visible region. By adopting polyomino subarray tiles quantization error can be minimized [6] [7], different approaches were employed to find optimal shape and position of the subarray tile. Nevertheless unequal subarrays increase the design and manufacturing complexity for mass production while square tiles are more attractive for their modularity. To mitigate grating lobes when using uniform subarrays amplitude tapering at subarray level is adopted [8] and different size can be employed to minimize the quantization error [9].

In this paper a subarray-based antenna is presented. The subarray is designed for Ka-band at f=19.95 GHz providing a simultaneous bandwidth of 500 MHz. Moreover the antenna supports the simultaneous left-hand and right-hand circular polarization (LHCP, RHCP). The paper is organized as follows: in Section 2 the antenna design is presented with a comparison between numerical simulations and measured fields from the manufactured prototypes. In Section 3 numerical simulations are presented showing performance of subarray tile in array, different scenarios for digital beamforming are considered in a comparison between fully-populated and subarray solution. Moreover integration of subarray tile with commercial beamformer is shown. Conclusions are drawn in Section 4.

2. Antenna Design

The design of a subarray-based antenna is presented in the following. A slot-fed patch antenna is firstly designed to satisfy the requirements listed in Tab. 1 in Ka-band. A slot-fed patch antenna, shown in Fig. 1 in the DLR's compact test anechoic chamber [10], is designed accordingly to the mathematical formulation provided by Milligan [11]. Rogers RT/duroid 6002 with Dk=2.94 is selected as material. The simultaneous RHCP and LCHP is achieved by means of a hybrid coupler 90° printed as stripline.

Frequency Range	19.7-20.2 [GHz]
Simultaneous bandwidth	500 [MHz]
Polarization	Simultaneous RHCP, LHCP
Boresight axial ratio	< 3 [dB]

Tab. 1. Requirements for the Ka antenna prototype.

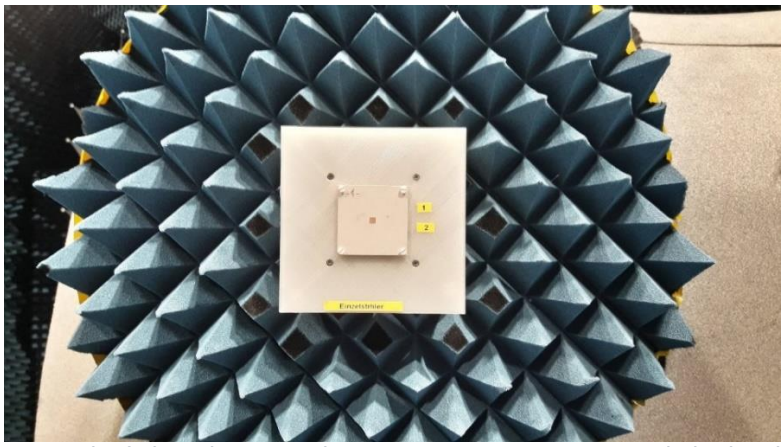

Fig. 1. Ka slot-fed patch antenna in DLR compact test range anechoic chamber.

As shown in Fig. 2, depicting the impedance matching in function of the frequency, it is worth to notice that simultaneous bandwidth of the patch antenna is more than 1 GHz. Moreover axial ratio in boresight direction, for both the polarizations, has kept a value below the 3 dB threshold for more than 1 GHz of bandwidth as represented in Fig. 3. Axial ratio in angular domain at the central frequency (f=19.95 GHz) is shown in Fig. 4(*a*)(*b*), the antenna exhibits good performance on a wide angular range. The radiated field of the slot-fed patch antenna is shown in Fig. 5, it is worth to mention a good matching with simulated results for both the polarizations.

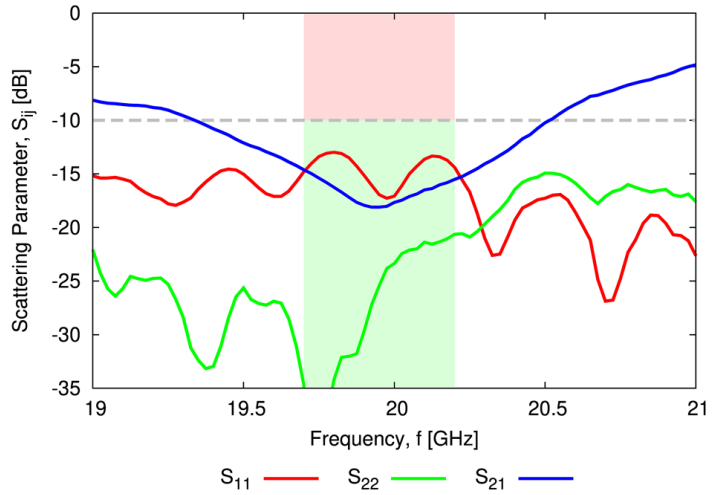

Fig. 2. Measured scattering parameters of dual-pol Ka slot-fed patch antenna prototype.

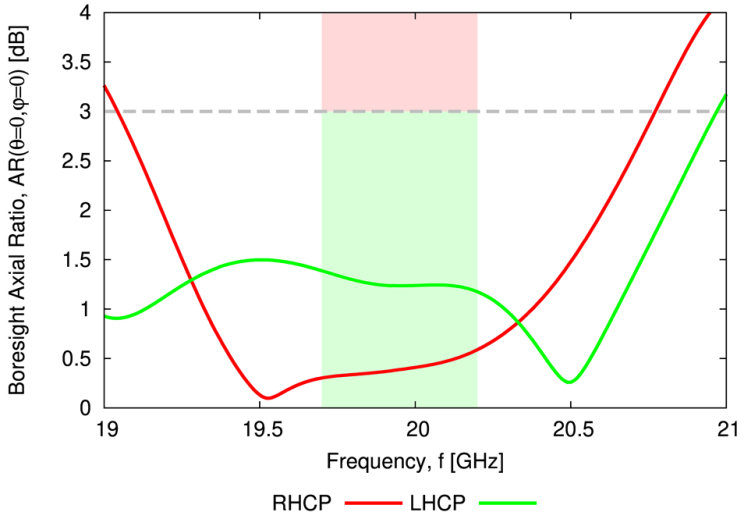

Fig. 3. Measured axial ratio of slot-fed patch antenna vs. frequency.

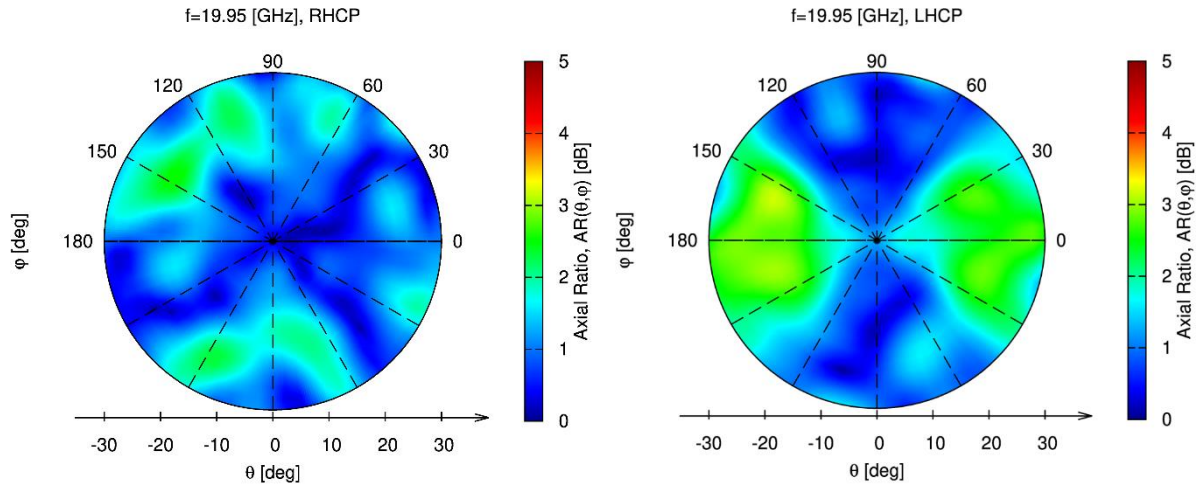

(*a*) (*b*)

Fig. 4. Measured axial ratio of slot-fed patch antenna in 3D angular domain for (*a*) RHCP and (*b*) LHCP polarization.

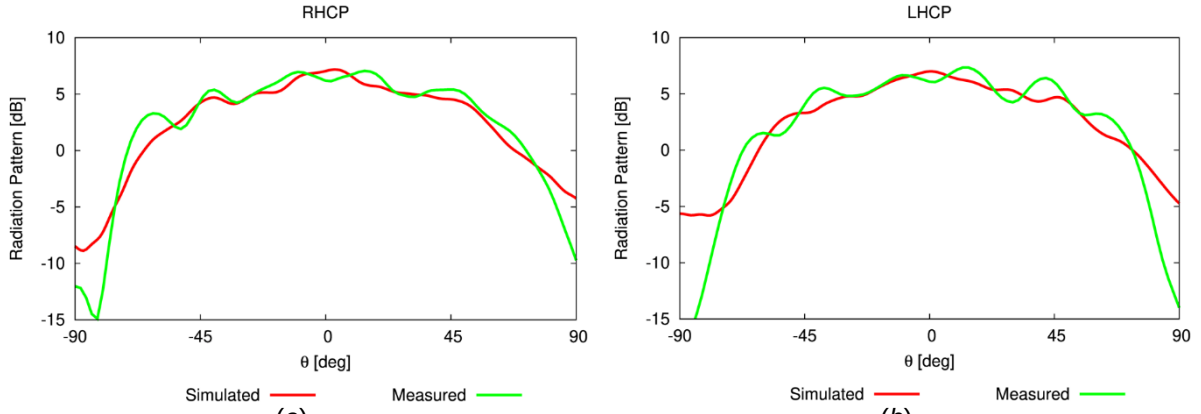

(*a*) (*b*)

Fig. 5. Simulated and measured radiated pattern [dB] of the slot-fed patch antenna for the (a) RHCP and (b) LHCP polarization.

A subarray, based on the patch antenna previously designed, is manufactured by clustering 16 elements in a shared TRM. As shown in Fig. 6, depicting the subarray prototype in anechoic chamber, the several patch antennas are equivalent to an unique antenna element with only one output port for polarization. The outcoming signal (RX mode) is then combined from the 16 patches with the same amplitude and phase.

As depicted in Fig. 7(*a*) the requirement on impedance matching is fully satisfied in the required bandwidth providing more than required 500 MHz. Also axial ratio in boresight direction, depicted in Fig. 7(*b*), has exhibited a high bandwidth covering around 2 GHz. Moreover the measured radiated field of the subarray antenna is shown in Fig. 8 in a comparison with simulated data in HFSS, it is worth to notice that there is a good match with full-wave simulations.

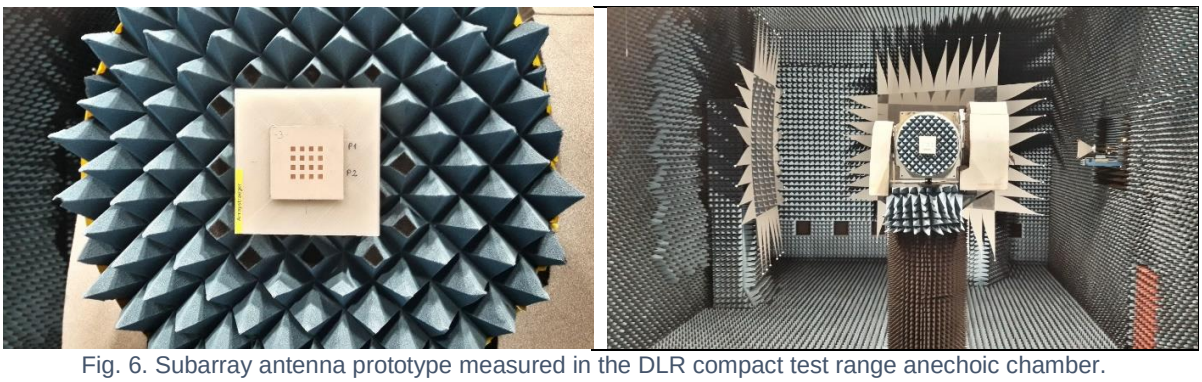

Fig. 6. Subarray antenna prototype measured in the DLR compact test range anechoic chamber.

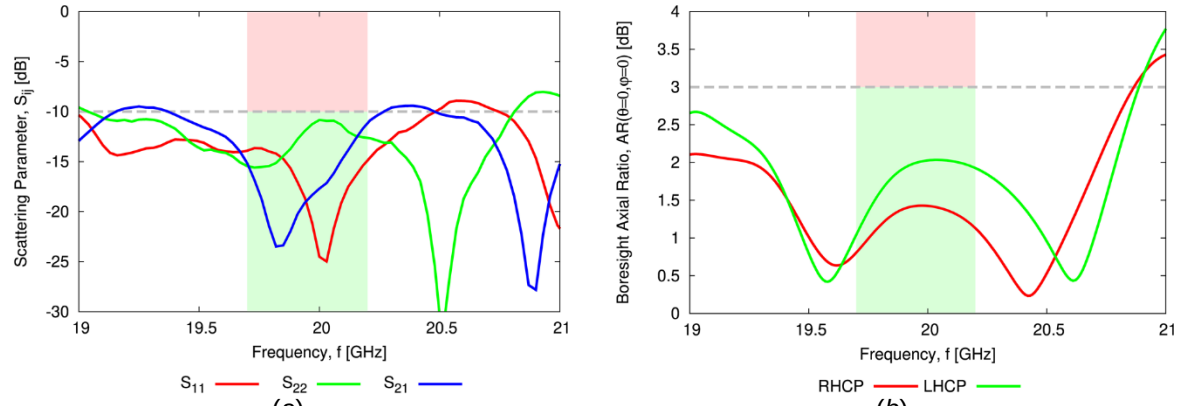

Fig. 7. Measured (*a*) scattering parameters and (*b*) axial ratio in boresight direction for the subarray antenna.

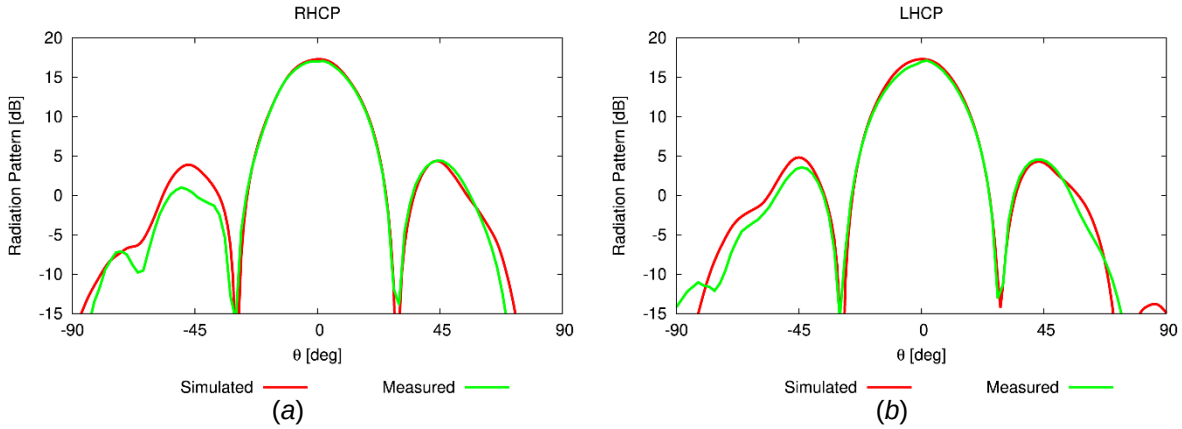

Fig. 8. Simulated and measured radiated pattern [dB] of the subarray for the (a) RHCP and (b) LHCP polarization.

3. Array Analysis

The previous designed subarray is considered in an array analysis. The radiated field of a phased array antenna is given by the analytical array factor formulation as [12]

$$F(\theta,\varphi)=\sum_{n=1}^{N} w_n e^{jk\{x_n\hat{u}+y_n\hat{y}+z_n\hat{w}\}} f_n(\theta,\varphi) \qquad (1)$$

where $w_n=\alpha_n e^{j\beta_n}$ is the complex excitations for the n-th element located in (x_n,y_n,z_n), $k=2\pi/\lambda$ is the wavenumber at the wavelength λ, $(\hat{u},\hat{v},\hat{w})$ is the direction cosine defined as $(\sin(\theta)\cos(\varphi),\sin(\theta)\sin(\varphi),\cos(\theta))$ and $f_n(\theta,\varphi)$ represents the embedded element pattern of the n-th element, when dealing with isotropic sources the term is omitted. In the following scenario $f_{n=1,\dots,N}(\theta,\varphi)=f_{sub}(\theta,\varphi)$ is considered uniform for all the elements (*i.e.* mutual coupling effects are not taken into account) where $f_{sub}(\theta,\varphi)$ is the far-field pattern radiated by the subarray.

The radiated field from the array is dependent on the element pattern, its spatial distribution and the weights w_n. Beamforming and beam steering is achieved by the proper selection of amplitudes and phases. For the steering case, only phases are changed accordingly to

$$\beta_n=-k(x_n\hat{u}+y_n\hat{y}+z_n\hat{w}) \qquad (2)$$

The developed subarray is taken as element for a bigger array, demonstrating electronic steering and digital beamforming for a real-time reconfiguration of the beam pattern.

An array of 36 subarray, corresponding to 576 patch antennas (*i.e.* 24x24), is considered. The array is placed in a square lattice grid with spacing 2λ at the central frequency. A comparison between 576-elements fully-populated array and 576-elements array based on subarray tiles is provided. Both arrays are excited with an uniform amplitude distribution and null phase. Radiation pattern for both arrays is shown in Fig. 9(*a*)(*b*) for respectively the fully-populated Fig. 9(*a*) and Fig. 9(*b*) subarray case.

Difference pattern is on the other hand achieved by applying a phase difference of 180 degrees among elements of different quadrants: the radiation pattern achieved by the fully-populated array is depicted in Fig. 9(*c*) while Fig. 9(*d*) shows the radiated field by using the 576-elements array based on subarray. It is worth to notice that subarray has permitted for the above mentioned scenarios to reduce the number of RF chains from 576 to 36 with similar performances. Finally, the 36-elements array based on subarray elements is simulated in a small steering range as shown in Fig. 10. For low sidelobe levels amplitude tapering techniques can be adopted together with square subarrays of different size to minimize quantization error and scan loss. Anyway in this analysis an uniform illumination is considered not being the goal of this work the synthesis analysis.

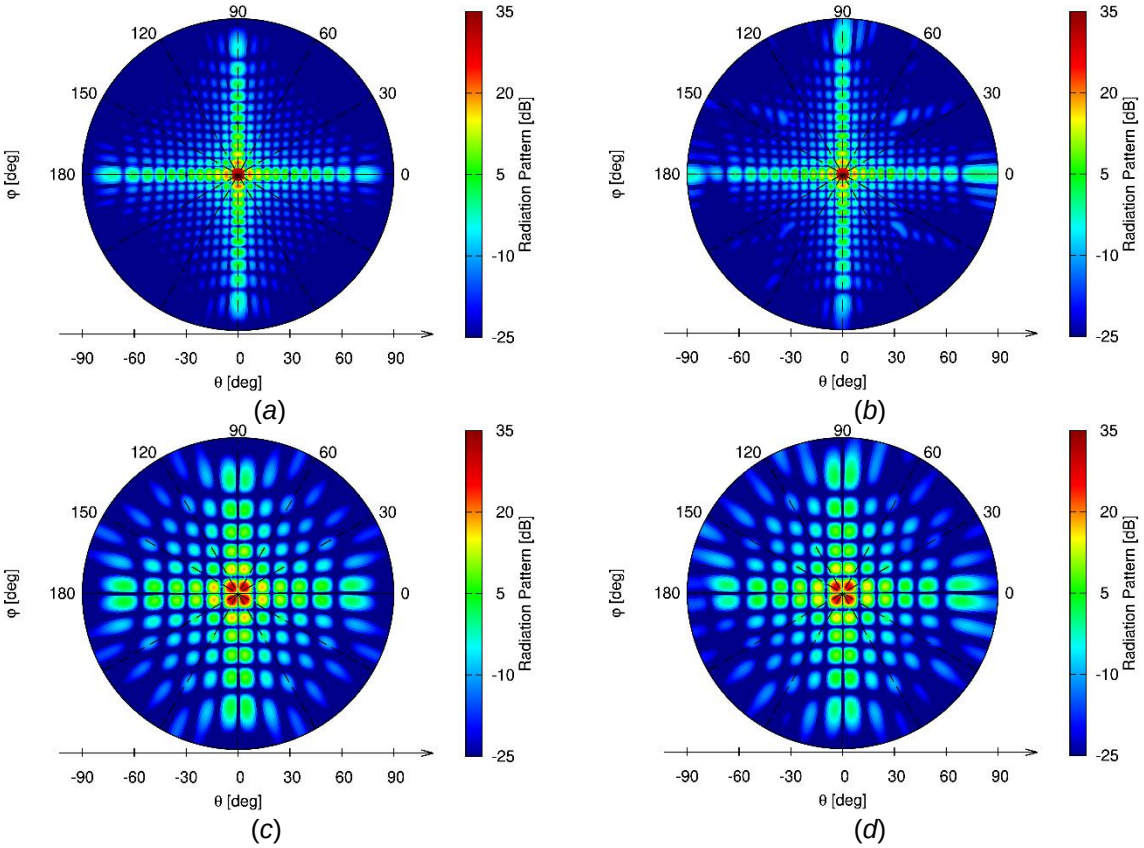

Fig. 9. (a)(b) Sum and (c)(d) difference pattern for an array of (a)(c) 576-elements fully-populated (b)(d) 36-elements based on subarray.

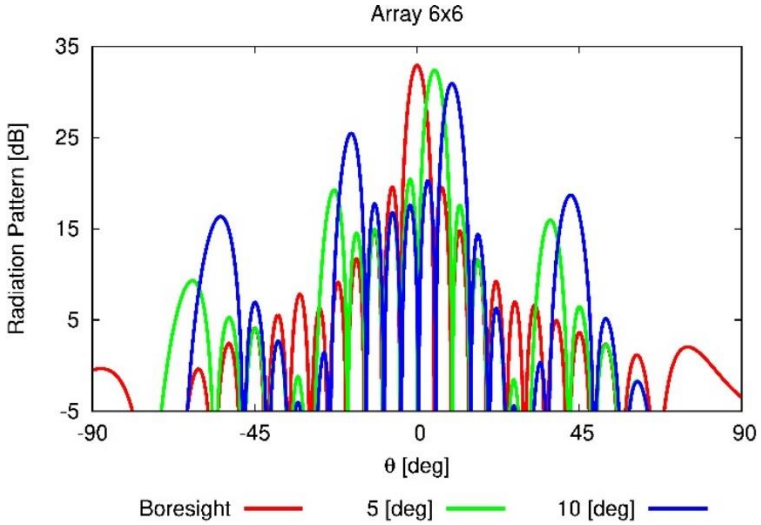

Fig. 10. Radiation pattern for the 36-elements array when steering is considered.

In order to control the antenna pattern with respect to direction of reception, sidelobe levels, etc., analog beamforming shall be employed. To achieve this the signals of several tiled subarrays shall be combined using a suitable beamformer. For the application at hand, a commercially available integrated circuit (IC), the Anokiwave AWMF-0132 has been considered. This device allows the combination of four receive signals in a frequency range from 17.7 to 20.2 GHz whereby the individual signal phases and amplitudes can be digitally controlled. The IC comes in a compact Wafer-Level Chip-Scale Package (WLCSP) which will facilitate later integration with the antenna PCB. In a first step, a development kit for the IC was used which is available from the manufacturer. This served to analyze the performance of the IC individually and to conduct beamforming tests with the antenna array without the need to integrate the two modules.
Fig. 11 shows the measurement setup of the beamforming IC development kit using a vector network analyzer (VNA). The measurements were used to assess any imbalances between the IC channels and to assess fitting beamforming coefficients for antenna pattern measurements. Moreover in Fig. 12 the beamforming IC is integrated with a modular 2x2 array testing the beamforming capabilities of the commercial chip with a compact version of the subarray presented in this paper and designed for modular arrays. In Fig. 12(*b*) the setup for the beamforming board integration is shown: 4 channels are connected to the 4 prototypes with one output, a SPI board is used with a LAN cable to program the chip on the positioner from the control room. Future works will present the results achieved in this phase that is currently under investigation.

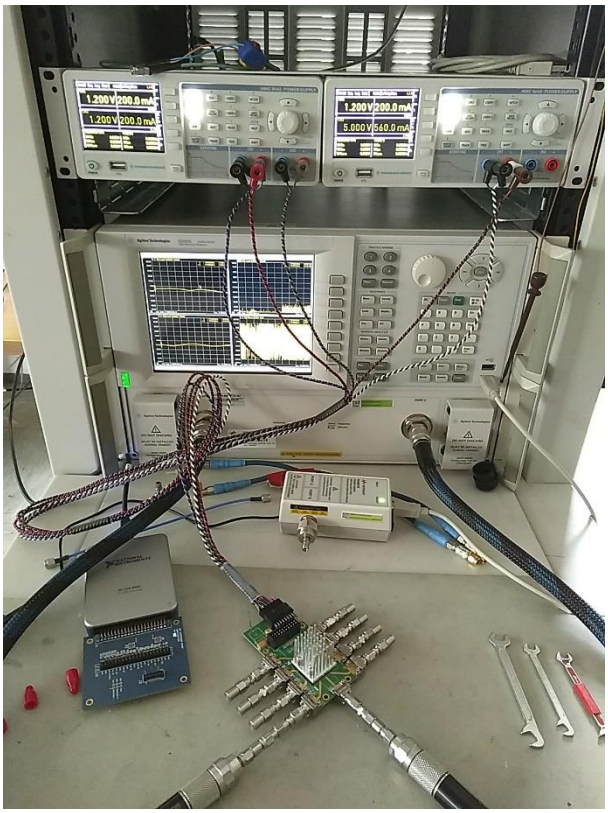

Fig. 11. Measurement of the beamforming IC with VNA.

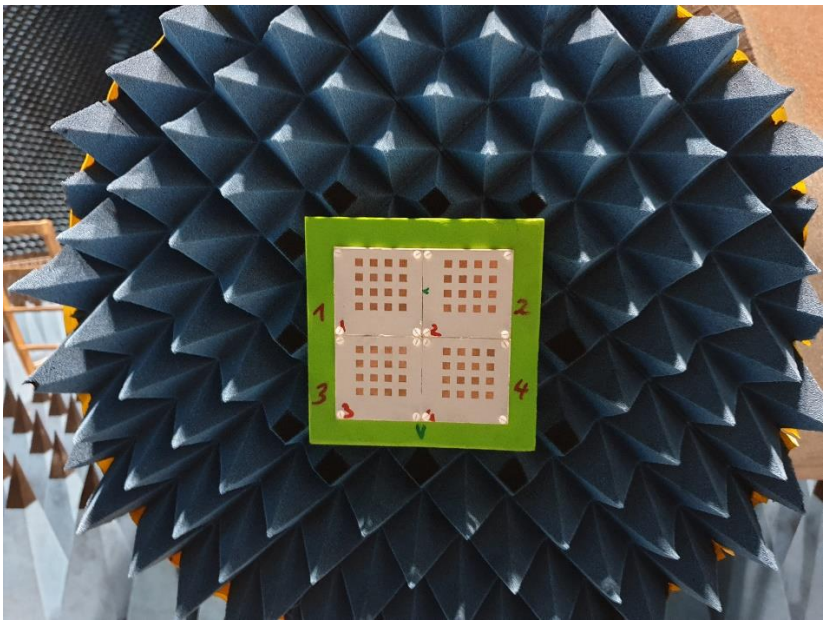

(*a*)

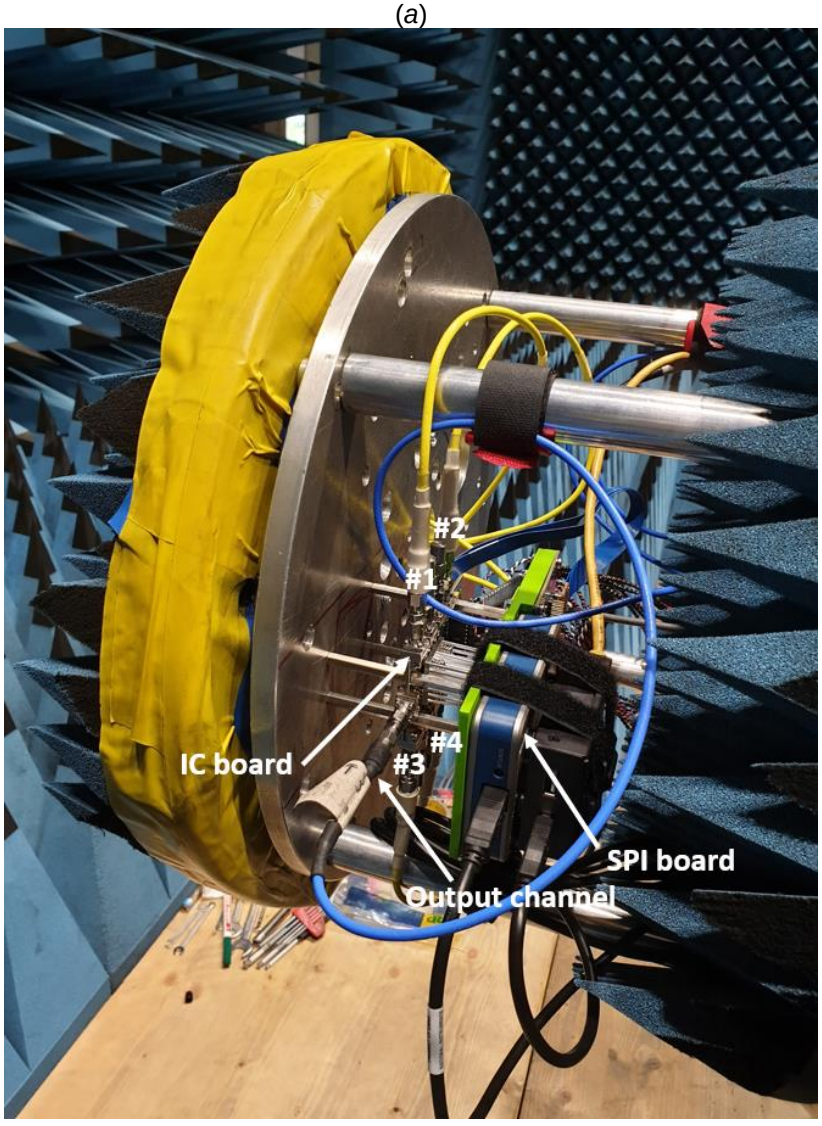

(*b*)

Fig. 12. Testing beamformer IC in anechoic chamber with a modular 2x2 array in the (*a*) front-view and (*b*) side-view.

4. Conclusion

In this paper we presented a prototype of subarray-based antenna developed at the Institute of Communications and Navigation of the German Aerospace Center (DLR) for Ka band. Measured results showed the capability to satisfy the requirements in terms of axial ratio and simultaneous bandwidth. Moreover an analysis of the suitability of the developed subarray prototype for bigger arrays was provided by considering an array of 36x36 elements as ground terminal in Ka band, achieving more than 30 dB of gain. In this first preliminary test the array appears to be well performing and fitting for allowing a reduction in terms of complexity, power consumption, final cost, weights and simplification for the mass production. Further work on the usability of subarray-based architectures for strong steering scenarios is still needed and is currently under investigation.

References

[1] R. L. Haupt, “Adaptively thinned arrays,” *IEEE Trans. Antennas Propag.,* vol. 63, no. 4, pp. 1626-1632, Apr. 2015.

[2] F. Boulos, L. Dall'Asta, G. Gottardi, M. A. Hannan, A. Polo, A. Salas-Sanchez, and M. Salucci, “A computational inversion method for interference suppression in reconfigurable thinned ring arrays,” *J. Phys.: Conf. Ser.,* vol. 1476, 2020.

[3] R. L. Haupt, “Thinned arrays using genetic algorithms,” *IEEE Trans. Antennas Propag.,* vol. 42, no. 7, pp. 993-999, Jul. 1994.

[4] N. Jin and Y. Rahmat-Samii, “Advances in particle swarm optimization for antenna designs: Real-number, binary, single-objective and multi-objective implementations,” *IEEE Trans. Antennas Propag.,* vol. 55, no. 3, pp. 556-567, Mar. 2007.

[5] W. P. M. N. Keizer, “Large planar array thinning using iterative FFT techniques,” *IEEE Trans. Antennas Propag.,* vol. 57, no. 10, pp. 3359-3362, Oct. 2019.

[6] R. J. Mailloux, S. G. Santarelli, T. M. Roberts, and D. Luu, “Irregular polyomino-shaped subarrays for space-based active arrays,” *Int. J. Antennas Propag.,* p. 956524, 2009.

[7] Z.-Y. Xiong, Z.-H. Xu, S.-W. Chen, and S.-P. Xiao, “Subarray partition in array antenna based on Algorithm X,” *IEEE Antennas Wireless Propag. Lett.,* vol. 12, pp. 906 - 909, Jul. 2013.

[8] R. Haupt, “Reducing grating lobes due to subarray amplitude tapering,” *IEEE Trans. Antennas Propag.,* vol. 33, no. 8, pp. 846-850, Aug. 1985.

[9] R. L. Haupt, “Optimized weighting of uniform subarrays of unequal sizes,” *IEEE Trans. Antennas Propag.,* vol. 55, no. 4, pp. 1207-1210, Apr. 2007.

[10] “DLR Compact Test Range,” [Online]. Available: https://www.dlr.de/hr/desktopdefault.aspx/tabid-6832/11242_read-26088/.

[11] T. A. Milligan, *Modern Antenna Design,* Hoboken, NJ, USA: Wiley, 2005.

[12] R. S. Elliott, *Antenna Theory & Design,* Hoboken, NJ, USA: Wiley, 2003.